Received: 28 January 2021 | Revised: 9 April 2021 | Accepted: 19 April 2021

DOI: 10.1096/fj.202100164R

RESEARCH ARTICLE

THE FASEB JOURNAL

Bisphosphonate inhibitors of squalene synthase protect cells against cholesterol-dependent cytolysins

Mateusz Pospiech[1] | **Siân E. Owens**[1] | **David J. Miller**[2] | **Karl Austin-Muttitt**[1] | **Jonathan G. L. Mullins**[1] | **James G. Cronin**[1] | **Rudolf K. Allemann**[2] | **I. Martin Sheldon**[1]

[1]Swansea University Medical School, Swansea University, Swansea, UK

[2]School of Chemistry, Cardiff University, Cardiff, UK

Correspondence
Mateusz Pospiech and I. Martin Sheldon, Swansea University Medical School, Swansea University, Swansea, UK.
Email: mateusz.pospiech@parisdescartes.fr (M.P.); i.m.sheldon@swansea.ac.uk (I.M.S.)

Present address
Mateusz Pospiech, Faculté de Pharmacie, CiTCoM, UMR 8038 – CNRS, Université de Paris, Paris, France

Funding information
Life Science Research Network Wales, Grant/Award Number: NRNS3APR009

Abstract

Certain species of pathogenic bacteria damage tissues by secreting cholesterol-dependent cytolysins, which form pores in the plasma membranes of animal cells. However, reducing cholesterol protects cells against these cytolysins. As the first committed step of cholesterol biosynthesis is catalyzed by squalene synthase, we explored whether inhibiting this enzyme protected cells against cholesterol-dependent cytolysins. We first synthesized 22 different nitrogen-containing bisphosphonate molecules that were designed to inhibit squalene synthase. Squalene synthase inhibition was quantified using a cell-free enzyme assay, and validated by computer modeling of bisphosphonate molecules binding to squalene synthase. The bisphosphonates were then screened for their ability to protect HeLa cells against the damage caused by the cholesterol-dependent cytolysin, pyolysin. The most effective bisphosphonate reduced pyolysin-induced leakage of lactate dehydrogenase into cell supernatants by >80%, and reduced pyolysin-induced cytolysis from >75% to <25%. In addition, this bisphosphonate reduced pyolysin-induced leakage of potassium from cells, limited changes in the cytoskeleton, prevented mitogen-activated protein kinases cell stress responses, and reduced cellular cholesterol. The bisphosphonate also protected cells against another cholesterol-dependent cytolysin, streptolysin O, and protected lung epithelial cells and primary dermal fibroblasts against cytolysis. Our findings imply that treatment with bisphosphonates that inhibit squalene synthase might help protect tissues against pathogenic bacteria that secrete cholesterol-dependent cytolysins.

KEYWORDS

bisphosphonate, cholesterol, cholesterol-dependent cytolysins, cytoprotection, pore-forming toxins, squalene synthase

Abbreviations: DCM, dichloromethane; DTT, dithiothreitol; ERK, extracellular-signal-regulated kinase; IPTG, isopropyl β-D-1-thiogalactopyranoside; JNK, c-Jun N-terminal kinases; MAPK, mitogen-activated protein kinases; MOPS, 3-morpholinopropane-1-sulfonic acid; PLO, pyolysin; SLO, streptolysin O; TMSBr, bromotrimethylsilane; ZA, zaragozic acid.

1 | INTRODUCTION

Pathogenic bacteria often secrete pore-forming toxins that cause leakage of cytosolic molecules, cytolysis, tissue damage, and disease in animals.[1] The most common class of pore-forming toxins are the cholesterol-dependent cytolysins. These cytolysins bind and form pores in cholesterol-rich areas of the plasma membrane of animal cells. The dependence of these cytolysins on cholesterol can be exploited because reducing cellular cholesterol can protect cells against damage.[2–5] This cytoprotection allows tissues to tolerate the presence of pathogenic bacteria that secrete cholesterol-dependent cytolysins.[3,4] However, as cholesterol is fundamental for cell physiology, it is challenging to find compounds that alter cellular cholesterol sufficiently to protect cells against cholesterol-dependent cytolysins, without adverse side effects on cell viability.

Pathogenic bacteria secrete cholesterol-dependent cytolysins as monomers, which assemble into multimers that insert into cholesterol-rich areas in plasma membranes to form β barrel pores.[1,2,6] These stable pores are about 30 nm diameter and lead to widespread changes in cells. There is initially membrane depolarization, leakage of potassium ions within 5 minutes of challenging cells with a cholesterol-dependent cytolysin, and activation of MAPK cells stress responses. Changes in cell shape occur within 15 minutes, accompanied by leakage of cytosolic proteins, such as lactate dehydrogenase (LDH), leading to reduced cell viability within 2 hours.[2,7–10] Commonly studied cytolysins include pyolysin produced by *Trueperella pyogenes*, which cause purulent diseases in farm animals, and streptolysin O produced by β-hemolytic group A *Streptococci*, which cause sore throats and impetigo in children.[11,12] In particular, pyolysin causes damage to endometrial epithelial and stromal cells, leading to postpartum uterine disease, which affects about 40% of dairy cattle annually.[2,13] Similarly, streptolysin O is thought to cause damage to the cells of the pharynx, contributing to the 37% of cases of pharyngitis associated with group A *Streptococci* in children over 5 years old.[14] Other diseases associated with cholesterol-dependent cytolysins include pneumonia, septicemia and meningitis caused by *Streptococcus pneumoniae*, which secretes pneumolysin; bacterial vaginosis caused by *Gardnerella vaginalis,* which produce vaginolysin; and gas gangrene caused by *Clostridium perfringens*, which secretes perfringolysin.[1,5,15–17] Pyolysin is particularly amenable to in vitro studies since it does not require thiol-activation, unlike most other cholesterol-dependent cytolysins.[18] Pyolysin and streptolysin O depend on accessible cholesterol to form pores in the plasma membrane of cells,[2,19] but pores only form when membranes contain >35 mol% cholesterol.[6,19] Thus, reducing cellular cholesterol is an attractive strategy to protect cells against these cytolysins and help animals tolerate pathogen.[13,20,21]

The abundance of cellular cholesterol partially depends on cholesterol biosynthesis, starting with the mevalonate pathway converting acetyl-CoA to the isoprenoid farnesyl diphosphate.[22] Statins inhibit the rate-limiting enzyme in the mevalonate pathway, HMG-CoA reductase, which reduces cholesterol biosynthesis, and can protect cells against cholesterol-dependent cytolysins.[3,23] However, statins also deplete isoprenoids in cells, and have side effects in patients, such as muscle cramps, prompting a search for other inhibitors of cholesterol biosynthesis. Squalene synthase catalyzes conversion of farnesyl diphosphate to squalene in the first committed step of cholesterol biosynthesis.[24] Inhibitors of squalene synthase include the fungus-derived zaragozic acids, and alkoxy-aminobenzhydrol derivatives, but none are in clinical use due to unfavorable toxicity profiles.[25–27] However, some nitrogen-containing bisphosphonates inhibit squalene synthase, and are likely to be safe because other bisphosphonates, which inhibit the enzyme that synthesizes farnesyl diphosphate, are safely used to treat osteoporosis.[28,29]

Here we tested the hypothesis that using bisphosphonates to inhibit squalene synthase would protect tissue cells against cholesterol-dependent cytolysins. The first step in our methodology was to design and synthesize bisphosphonates that inhibit squalene synthase. We then used epithelial cells, which are often the first point of contact with pathogens, to screen the bisphosphonates for cytoprotection against cholesterol-dependent cytolysins and to identify a lead molecule. Finally, we examined the ability of the lead molecule to protect other tissue cells against the damage caused by cholesterol-dependent cytolysins.

2 | METHODS

2.1 | General procedures for synthesis of nitrogen-containing bisphosphonates

The chemicals used for synthesis were analytical quality or better, and purchased from Sigma-Aldrich (Gillingham, Dorset, UK), Apollo Scientific (Stockport, Cheshire, UK) and Thermo Fisher Scientific (Loughborough, UK). Reactions were carried out in an inert atmosphere of argon. All glassware was cleaned with acetone and water and dried in the oven before use.

Tetralkyl esters of N-substituted aminobisphosphonates were designed based on previously synthesized compounds that inhibit squalene synthase,[30,31] and prepared using two methods described previously.[32,33]

Method A.[32] To a cold solution (ice/NaCl bath −10°C) of isonitrile and (0.050 mol, 1 eq), triethyl phosphite (0.1 mol, 2 eq) in 100 mL dichloromethane (DCM), cold (−10°C) 4 M HCl (0.15 mol in 1,4-dioxane) was added dropwise and the reaction mixture was stirred for approximately 1.5 hours

(Figure 1A). The resulting reaction mixture was further diluted by addition of another portion of 100 mL DCM and then reaction mixture was washed with a cold (0°C) solution of 5 × 100 mL saturated $NaHCO_3$. The organic phase was collected and dried over anhydrous Na_2SO_4, solution filtered, and the solvent removed under reduced pressure to give

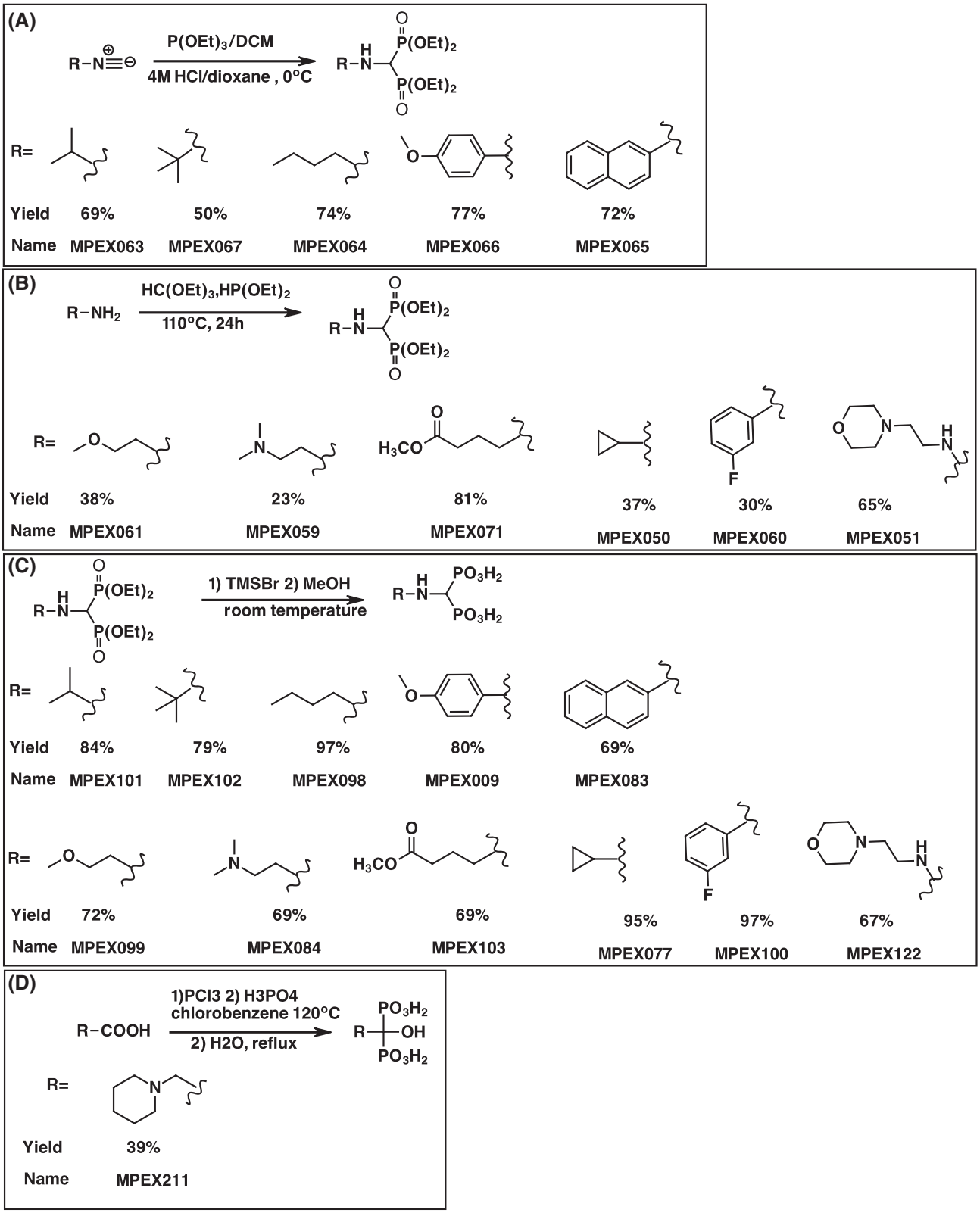

FIGURE 1 Synthesis of nitrogen-containing bisphosphonates. A, Synthesis of N-substituted aminomethylidenebisphosphonates from isonitriles.[27] B, Synthesis of tetraethyl bisphosphonates from amines.[29] C, Acids resulting from the hydrolysis.[30] D, Synthesis of PHPBP, a reference inhibitor

yellow to dark brown oil as described further in Supporting Information Figure S1.

Method B,[33] a mixture of amine (Figure 1B), triethyl orthoformate and diethyl phosphite was stirred at 110°C for 24 hours. The reaction mixture was cooled, and the volatiles removed under reduced pressure.

Hydrolysis of the bisphosphonate tetraesters was carried out following the McKenna procedure.[34] Neat bromotrimethylsilane (TMSBr, 15 eq) was added dropwise to the tetraester and the resulting mixture was stirred for 24 hours at room temperature; subsequently volatiles were removed in vacuo and resulting residue was dissolved in methanol and stirred at room temperature for 1 hour. Solvent was removed under reduced pressure and the resulting typically white solid was recrystallized.

Compounds were characterized by ^{1}H, ^{13}C, ^{31}P and ^{19}F NMR spectra analyzed with Avance 400 or Avance 300 NMR spectrometers (Bruker, Coventry, UK); and, mass spectra analyzed using an LCT Premier XE spectrometer (Waters, Elstree, Hertfordshire, UK) fitted with a 1525 Micro binary HPLC pump. Compound characterization is presented in Supporting Information Figure S1.

2.2 | Protein expression and purification

Plasmid pET21d-His harboring a gene for human squalene synthase containing a N-terminal hexa-histidine-tag (Epoch, Missouri City, Texas) was transformed in BL21-CodonPlus (DE3)-RP competent bacteria (Agilent Technologies, Santa Clara, CA) and incubated overnight at 37°C. One colony was inoculated in 10 mL Luria Broth with 100 mg/L ampicillin overnight at 37°C, and then inoculated into 3 L Terrific Broth with 100 mg/L ampicillin and incubated with shaking at 250 rpm at 37°C until 0.6 to 0.8 OD_{600} was reached. The flask was cooled to 4°C for 1 h, and expression of squalene synthase induced using IPTG (120 mg/L, isopropyl β-D-1-thiogalactopyranoside) with shaking at 250 rpm for 2 d at 16°C. The bacteria were pelleted by centrifugation at 22,790 × *g* for 30 minutes at 4°C (Sorvall RC5B centrifuge), and stored at −20°C. Cell pellets were resuspended in 50 mM 3-morpholinopropane-1-sulfonic acid (MOPS buffer, pH 7.2) with 0.5% sodium deoxycholate, disrupted by sonication (40% amplitude for 3 minutes with 5 s on/10 s off cycles), and centrifuged at 22,790 ×*g* for 25 minutes. The supernatant was discarded, and protein recovered by adding MOPS buffer containing 1% Tween 80, and then 1 M NaOH until the solution became clear. The solution was stirred at 4°C for 30 minutes before addition of 2-mercaptoethanol, and 1 M HCl to pH 7.2. The suspension was centrifuged at 22,790 ×*g* for 30 minutes, and the supernatant loaded into a 0.5 mL Ni-NTA column equilibrated with buffer (50 mM MOPS, 30 mM NaCl, 20 mM imidazole, pH 7.2) and eluted using a 20 to 500 mM imidazole gradient. Following SDS-PAGE analysis, fractions containing squalene synthase (47 kDa) were pooled and concentrated to a final volume of ~3 mL using a Microcon 30 kDa centrifugal filter unit with Ultracel-30 membrane (Merck, Watford, Hertfordshire, UK). The concentrate was then dialyzed with 50 mM phosphate buffer containing 1% Tween 80, 2% isopropanol, 10 mM $MgCl_2$ and 1 mM 1,4-dithiothreitol. The concentration of protein was measured using a Bradford Assay (Thermo Fisher Scientific, Waltham, MA), according to the manufacturer's instructions.

2.3 | Squalene synthase activity assay

The assay used for enzyme activity was modified from previously described methods.[35–37] Each assay contained 50 mM phosphate (pH 7.4), 10 mM $MgCl_2$, 1% (v/v) Tween-80, 10% (v/v) 2-propanol, 1 mM DTT, 1 mg/ mL BSA, 1 mM NADPH, farnesyl diphosphate and 0.1 μM squalene synthase in a total volume of 200 μL in 1 mL eppendorfs. Reactions were pre-incubated at 37°C without the substrate for 10 minutes, and then another 10 minutes after addition of ^{3}H-farnesyl diphosphate. [1-^{3}H]-farnesyl diphosphate (20 Ci/mMol, American Radiolabeled Chemicals, Saint Louis, USA) was diluted by adding cold farnesyl diphosphate to give final activity around 24 000 dpm/μM. Reactions were quenched with 40% KOH solution in water/methanol 1/1 (v/v). Solid NaCl was added to saturate the mixture. The mixture was then extracted with 3 × 1 mL of hexane containing 0.5% (v/v) squalene and extracts were passed through a short pipette column containing silica gel. The column was washed with 1 mL of toluene containing 0.5% (v/v) squalene. The radioactivity of the eluent was measured in 15 mL scintillation cocktail (Opti-Fluor purchased from Perkin Elmer) using a QuantaSmart scintillation counter (Perkin Elmer).

The inhibitory activity of synthesized nitrogen-containing bisphosphonates against squalene synthase was determined by incubation with [squalene synthase] = 0.5 μM, [NADPH] = 1 mM, [1-^{3}H]- farnesyl diphosphate = 10 μM for 10 minutes at 37°C in the range of concentrations of 0.1 nM – 100 μM. Steady-state kinetic parameters of squalene synthase were measured by incubation with [squalene synthase] = 0.1 μM, [NADPH] = 1 mM, and range of concentrations of [1-^{3}H]- farnesyl diphosphate = 0-40 μM for 10 minutes at 37°C (Supporting Information Figure S2). The k_{cat} and K_M were found to be 0.0024 s^{-1} and 3.36 μM respectively. Thompson *et al*. 1998 measured steady state kinetic parameters using the same methodological approach and received K_M values between 1 and 2.8 μM which differ slightly to those reported here.[35] Differences between steady state kinetic parameters based on the method used have been reported for other terpene synthases.

2.4 | In silico docking studies

In silico docking studies were performed using a combination of empirical and force-field approaches incorporated within an in-house pipeline called "Shipyard", which is used for high throughput virtual screening of protein-ligand dockings. The structure of human squalene synthase was obtained from the RCSB Protein Data Bank (PBD, 3VJC) in complex with zaragozic acid. The squalene synthase protein structure and cofactors were prepared using the Chimera software to correct inconsistencies in the structure including the removal of solvent and crystallization additives.[38] Protonation and partial charge calculations for each residue and cofactor were undertaken using the Antechamber software,[39] a mapping of all pockets and grooves was generated using Sphgen,[40] and the electrostatic field in the 3D volume of squalene synthase was pre-calculated with GRID.[41] The binding pockets of squalene synthase were determined using DoGSiteScorer.[42] Output of the binding site search was verified manually via comparison with the original crystal structure. All ligand structures were subjected to the Open Babel system to make hydrogen atoms explicit,[43] and the Balloon package was used to generate minimal-energy 3D structures,[44] with partial charges assigned to each ligand.[45]

To generate the 10 best poses for ligands in the squalene synthase protein docking was performed using DOCK 6[46] and AutoDock Vina,[47] which assign a binding energy score and rank, alongside the DrugScoreX atom distance profile affinity calculations. Further physicochemical docking parameters were analyzed to investigate simulated squalene synthase-ligand interactions in more detail (Table 1, Supporting Information Table S1). Parameters most closely associated with the strong interactions observed with the positive controls were identified to provide further insight into potential mechanisms of interaction. Images of best poses of selected candidates were generated in Chimera.

2.5 | Cell culture

Experiments used newly purchased HeLa cervical epithelial cells (ATCC CCL-2, ATCC, Manassas, VA, USA), A549 lung epithelial cells (ATCC CCL-185), and primary normal human dermal fibroblasts (C-12302, Promocell, Heidelberg, Germany). Cells were cultured in 75 cm^2 tissue culture flasks (Greiner Bio-One, Stonehouse, UK) with complete culture medium, incubated at 37°C in humidified air with 5% CO_2, and passaged every 2 to 3 days. Complete culture medium for HeLa cells comprised DMEM (Thermo Fisher Scientific, Perth, UK) supplemented with 10% fetal bovine serum and 1% antibiotic antimycotic solution (Sigma-Aldrich), and for A549 cells comprised RPMI1640 (Thermo Fisher Scientific) supplemented with 5% fetal bovine serum, 1% antibiotic antimycotic solution and 1% glutamine (Sigma-Aldrich). Complete culture medium for dermal fibroblasts comprised Fibroblast Growth Medium 2 with supplement mix (Promocell).

The HeLa and A549 cells were seeded at 50,000 cells/mL and dermal fibroblasts at 14,000 cells/mL, using 1 mL/well complete culture medium in 24-well culture plates (TPP, Trasadingen, Switzerland]. When cells were 90% confluent, medium were replaced with serum-free culture medium containing vehicle or treatments, and for the durations specified in *Results*. Treatments were the synthesized nitrogen-containing bisphosphonates, or zaragozic acid, atorvastatin, alendronate, methyl-β-cyclodextrin, farnesyl diphosphate or geranylgeranyl diphosphate (all Sigma-Aldrich). The cells were then challenged with serum-free control medium or

TABLE 1 Squalene synthase inhibition

Inhibitor name	Formula	Molecular weight	Inhibition of squalene synthase by acid	Inhibition of squalene synthase by ester
MPEX009	$C_8H_{12}NO_7P_2$	297	No	No
MPEX077	$C_4H_{10}NO_6P_2$	231	No	No
MPEX083	$C_{11}H_{13}NO_6P_2$	340	No	No
MPEX084	$C_5H_{15}N_2O_6P_2$	262	No	No
MPEX098	$C_5H_{15}NO_6P_2$	247	Yes	No
MPEX099	$C_4H_{13}NO_7P_2$	249	Yes	No
MPEX100	$C_7FH_{10}NO_6P_2$	285	No	No
MPEX101	$C_4H_{12}N0_6P_2$	233	No	No
MPEX102	$C_5H_{14}NO_6P_2$	247	No	No
MPEX103	$C_{15}H_{19}NO_6P_2$	371	No	No
MPEX122	$C_7H_{16}N_2O_7P_2Na_4$	394	No	No
MPEX211	$C_8H_{19}NO_7P_2$	303	Yes	Not applicable

Note: n = 23. Inhibitory activity of synthesized bisphosphonic acids and corresponding esters against human squalene synthase in a cell-free system.

medium containing pyolysin or streptolysin O, in the concentrations and durations specified in *Results*. Pyolysin was generated from the pGS59 plasmid (a generous gift from Prof BH Jost, University of Arizona, USA), as described previously.[2] Streptolysin O was purchased and used following the manufacturer's instructions (Sigma-Aldrich). At the end of the experiment, supernatants were collected and stored at 4°C for measurement of LDH, and cell viability was measured as described below.

For measurement of cholesterol, potassium, or proteins by Western blot, HeLa or A549 cells were seeded at 50,000 cells/mL in 3 mL complete culture medium in 6-well plates (TPP). When cells were 90% confluent, media were replaced with serum-free culture media containing vehicle, MPEX098, zaragozic acid or methyl-β-cyclodextrin for 24 hours, and the cells were then challenged with control serum-free medium or medium containing pyolysin or streptolysin O, in the concentrations and durations specified in *Results*. Total cellular cholesterol was measured using the Amplex Red Cholesterol Assay Kit (Thermo Fisher Scientific), and abundance normalized to protein abundance (DC assay, Sigma-Aldrich), according to the manufacturers' instructions. For the measurement of potassium, the cells were washed three times with choline buffer (pH 7.4, 120 mM choline chloride, 0.8 mM $MgCl_2$, 1.5 mM $CaCl_2$, 5 mM citric acid, 5.6 mM glucose, 10 mM NH_4Cl, 5 mM H_3PO_3, all Sigma-Aldrich), and then challenged with choline buffer (control) or choline buffer containing pyolysin. The supernatants were collected after 10 minutes and potassium measured using a Jenway PFP7 flame photometer, according to the manufacturer's guidelines. For Western blotting, cells were collected in PhosphoSafe Extraction Reagent (Merck, Watford, Hertfordshire, UK) and stored at −20°C.

2.6 | Cell viability and LDH assay

The viability of HeLa and A549 cells was evaluated using the MTT assay, as described previously.[48] Briefly, cells were incubated for 2 hours with 1 mg/mL MTT (tetrazolium dye 3-(4,5-dimethylthiazol-2-yl)-2,5-diphenyltetrazolium bromide, Sigma-Aldrich] in serum-free medium. Supernatants were removed, cells lysed using 300 µL/well DMSO, and optical density measured (OD_{570}) using a POLARstar Omega plate reader (BMG Labtech, Ortenberg, Germany). The viability of dermal fibroblasts was evaluated by incubating cells for 6 hours with the Alamar Blue Cell Viability Reagent (Thermo Fisher Scientific), and the enzymatic reduction of resazurin to resorufin measured using a POLARstar Omega microplate reader (540/580 nm excitation/emission).

The activity of LDH in cell culture supernatants was measured as described for the Lactate Dehydrogenase Activity Assay Kit (Sigma-Aldrich). Briefly, as LDH catalyzes conversion of lactate to pyruvate, the reduction of NAD^+ to NADH is quantified by conversion of iodonitrotetrazolium chloride to red formazan, using phenazine methosulphate as an electron carrier. Standards (0, 5, 10, 15, 20, 25 nmoles NADH) or samples were added in duplicate to a 96-well half-area plate (Greiner Bio-One, 20 µL/well), with 30 µL/well buffer (0.2 M Tris buffer, pH 8.2). To initiate the reaction, 50 µL freshly prepared assay mix (54 mM lactate, 0.66 mM iodonitrotetrazolium chloride, 0.28 mM phenazine and 1.3 mM NAD^+ in 0.2 M Tris buffer, pH 8.2; all Sigma) was added to each well. The OD_{450} was measured using a POLARstar Omega plate reader, initially and following incubation at 37°C for 30 minutes, and LDH activity calculated following the manufacturer's instructions.

2.7 | Western blotting

Samples were diluted to 20 µg/mL in a 1:5 ratio with Laemelli sample buffer, heated for 10 minutes at 95°C, and subjected to SDS-PAGE on a 12% polyacrylamide gel, using All Blue Prestained Protein Standards (Bio-RAD, Watford, Hertfordshire, UK). Proteins were transferred to Hybond P 0.45 µm PVDF membrane (Fisher Scientific), blocked for 1 hour in blocking buffer (5% BSA, 20 mM Tris pH 7.6, 137 mM NaCl and 0.1% v/v Tween 20; all Sigma-Aldrich), and then incubated overnight at 4°C in blocking buffer with 1:1000 dilution of primary antibody for total and phosphorylated JNK, p38, and ERK (Supporting Information Table S2). The membrane was washed 5× in wash buffer (20 mM Tris pH7.6, 125 mM NaCl, 0.1% v/v Tween 20) and bound antibodies identified by incubation for 1 hour at room temperature with 1:1000 HRP-linked anti-mouse IgG or anti-rabbit IgG (Cell Signaling Technology Inc, Danvers, MA, USA), washed 5× in wash buffer, and visualized by chemiluminescence (Clarify Western ECL Substrate, Bio-RAD) and a BIO-RAD ChemiDoc XRS system. The membrane was stripped using Restore Western Blot Stripping Buffer (Thermo Fisher Scientific) to detect another MAPK, or alpha-tubulin (New England Biolabs, Hitchin, Hertfordshire, UK). The density of protein bands was analyzed by ImageJ.

2.8 | Cell imaging

Cells were plated at a density of 50,000/mL for HeLa and 14,000/mL for dermal fibroblasts on coverslips in 24-well plates, and incubated for 24 hours (HeLa) or 48 hours (dermal fibroblasts) in complete culture medium at 37°C in humidified air with 5% CO_2. Cells were washed three times with PBS, fixed with 4% paraformaldehyde, washed three times, and permeabilized with 0.2% Triton X-100 in PBS. Cells were then washed three times in PBS and blocked with

0.1% Triton X-100 with 1% BSA in PBS for 1 hour, and subsequently probed with 1:1000 Alexa Fluor 555 Phalloidin (Thermo Fisher Scientific) in blocking buffer to visualize actin, or 50 μg/mL filipin III from *Streptomyces filipinensis* (Sigma-Aldrich) to visualize cholesterol within the cellular membranes.[49] Cells were washed three times in PBS and coverslips mounted on slides using mounting medium with DAPI (Vector Laboratories Inc; Burlingame, CA). Cell morphology and actin localization were analyzed with an Axio Imager M1 upright fluorescence microscope (Zeiss, Jena, Germany) and images captured using an AxioCamMR3. Cell cholesterol was analyzed using a LSM710 confocal microscope (Zeiss) with the Zeiss Zen 2010 software. Images were captured using an 63x oil objective using the channel range 410 to 476 nm. The coverslips were subjected to identical exposure times and conditions.

2.9 | Statistical analysis

Data are presented as mean (SEM). The statistical unit was the independent cell passages for each experiment. Statistical analyses were performed using Prism 7 (GraphPad Software, San Diego, CA), with significance ascribed when $P < .05$. Data were examined for normality and normally distributed data analyzed by student's *t* test, or ANOVA with Dunnett's or Sidak post-hoc tests, as reported in *Results*. Non-parametric data were explored using the Mann-Whitney test, multiple *t* test with Holm-Sidak post hoc test, or Kruskal-Wallis test with Dunn's post hoc test, as specified in *Results*

3 | RESULTS

3.1 | Synthesis of nitrogen-containing bisphosphonates

We designed nitrogen-containing bisphosphonates that we predicted might inhibit squalene synthase based on established bisphosphonates that inhibit squalene synthase,[30,31] and that were tractable for laboratory synthesis.[32,33] The bisphosphonates were synthesized using two different strategies. First, tetralkyl esters of N-substituted aminobisphosphonates were prepared using the method previously described by Goldeman et al (Figure 1A).[32] Briefly, isonitriles were converted to isonitrilium salts by the addition of 4 M HCl solution in 1,4-dioxane, reacted with triethylphosphite to create the intermediate phosphonium salt, which transforms into diethyl N-substituted iminomethylidenephosphonate, and then undergoes an Arbuzov-like reaction to yield triethyl N-substituted aminomethylidenebisphosphonate.[32,50] Although the reaction is completed within 2 hours at temperatures as low as 0°C, few isonitriles are available commercially and so our second strategy was to use the method described previously by Suzuki et al (Figure 1B).[33] Briefly, primary amines were treated for up to 24 hours with triethylorthoformate and diethyl phosphite at 110°C to yield tetraethyl bisphosphonates. Bisphosphonate tetraesters synthesized following both strategies were then hydrolyzed using bromotrimethylsilane (Figure 1C).[51] Briefly esters were treated with excess bromotrimethylsilane for 24 hours at room temperature, and the resulting residue was treated with methanol for 1 hour to yield bisphosphonic acids.[34] A reference squalene synthase inhibitor, 3-(1-piperidino)-1-hydroxypropylidene-1,1-bispho sphonic acid (also known as PHPBP, Figure 1D; MPEX211), was synthesized as described previously.[30,51]

3.2 | Bisphosphonates inhibition of human recombinant squalene synthase

Squalene synthase activity was examined using a cell-free system and supplying tritiated farnesyl diphosphate (Supporting Information Figure S2). The ability to inhibit human squalene synthase was determined for the 11 synthesized bisphosphonic acids, their 11 corresponding esters, and MPEX211 (Table 1). The IC_{50} of the effective inhibitors was measured, using MPEX211 as a reference compound with a previously reported IC_{50} of 0.31 μM.[30] In the present study, the IC_{50} for MPEX211 was 0.35 μM, for MPEX099 was 2.42 μM, and for MPEX098 was 0.41 μM (Supporting Information Figure S3).

3.3 | In silico docking analysis

We used in silico ligand docking to further validate binding of the nitrogen-containing bisphosphonates to the active site of squalene synthase. Scores for compounds docking to squalene synthase (Table 2) were generated using a combination of empirical and force-field molecular docking approaches, applied to the protein structure and active site provided by the crystal structure of human squalene synthase in complex with zaragozic acid (3VJC, resolution 1.89 Å, RCSB Protein Data Bank). Computer simulations indicated strong interactions between squalene synthase and established squalene synthase inhibitors, zaragozic acid (Figure 2A), lapaquistat (TAK-475, Figure 2B) or RPR107393 (Figure 2C). Among the nitrogen-containing bisphosphonates synthesized in the present study, there were also strong interactions between squalene synthase and MPEX098 or MPEX211 (Figure 2D,E), but not MPEX101 or MPEX102 (Figure 2F,G). We particularly focused on the DSX per contact score (Table 2), which is a knowledge-based scoring function that measures a basket of distance-dependent pair potentials, novel torsion angle

TABLE 2 Docking scores

Compound	Electrostatics	Solvation	Vina_ Gauss_2	Bond_Entropy	DSX_Contact_ count	DSX_Per_ contact
Zaragozic acid	0.893	35.261	−10.007	9.193	−124.243	−0.156
TAK-475	2.355	30.972	−9.373	4.795	−112.592	−0.168
RPR107393	5.901	8.745	7.218	1.530	−102.991	−0.178
MPEX098	−45.359	72.648	−4.188	2.350	−51.049	−0.143
MPEX211	−27.600	66.359	−5.069	2.834	−70.083	−0.152
MPEX101	−53.635	76.086	−3.945	1.956	−42.173	−0.120
MPEX102	−50.485	77.032	−4.162	1.798	−33.102	−0.092

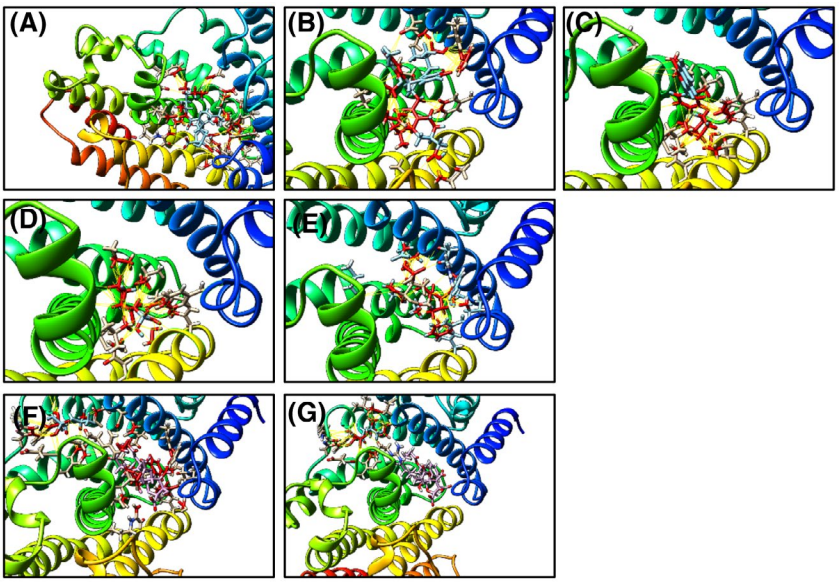

FIGURE 2 In silico docking analysis. Images indicating docking outcomes using Chimera software with indicated point of contact marked by yellow lines. Docking shows established squalene synthase inhibitors, zaragozic Acid (A), TAK-475 (B) RPR107393 (C); synthesized nitrogen-containing bisphosphonates MPEX098 (D), MPEX211 (E), MPEX101 (F), and MPEX102 (G)

potentials and solvent accessible surface-dependent potentials.[52] The highest scores were derived for zaragozic acid, lapaquistat, and RPR107393, followed by MPEX098 and MPEX211. Markedly lower scores were attained with MPEX101 and MPEX102.

3.4 | Screening for cytoprotection against cholesterol-dependent cytolysins

To screen the bisphosphonates for cytoprotection against cholesterol-dependent cytolysins, we first established in vitro cell models that were sensitive to cytolysins. Challenging HeLa or A549 epithelial cells with pyolysin or streptolysin O for 2 hours produced a concentration-dependent reduction in cell viability, as determined by MTT assay, and an increase in pore formation, as determined by the leakage of LDH into cell supernatants (Figure 3; ANOVA, $P < .001$). For subsequent cytoprotection studies we used 2.5 μg/mL pyolysin and 9.4 μg/mL streptolysin O for HeLa cells, and 1.3 μg/mL pyolysin and 9.4 μg/mL streptolysin O for A549 cells, because these concentrations reliably caused cytolysis. We used a 2 hours challenge because the aim was to evaluate protection against cytolysins, rather than the ability of cells to recover after damage.

To screen for cytoprotection against cholesterol-dependent cytolysins, HeLa cells were treated for 24 hours with serum-free media containing 1 mM of each synthesized nitrogen-containing bisphosphonic acid or tetraester. The treatment media were removed, and the cells were then challenged for 2 hours with control medium or medium containing 2.5 μg/mL pyolysin, and cell viability determined by MTT assay and pore formation estimated by measuring the leakage of LDH into cell supernatants (Figure 4). Five bisphosphonates were cytoprotective against pyolysin with cell viability > 50% compared with the vehicle treatment challenged with control (Figure 4A), and with LDH leakage < 50% of the vehicle treatment challenged with pyolysin (Figure 4B; data not shown for three compounds that caused cytotoxicity per se).

Among the five cytoprotective candidate bisphosphonates, only MPEX098 inhibited squalene synthase in the cell-free assay (Supporting Information Figure S3), docked

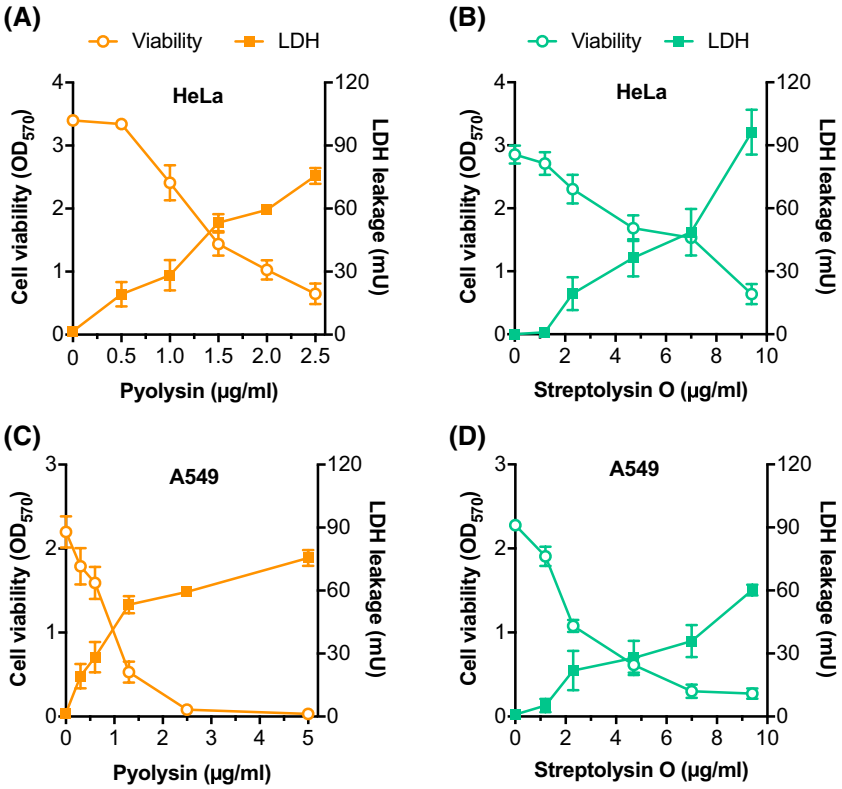

FIGURE 3 Cellular sensitivity to cholesterol-dependent cytolysins. HeLa cells (A, B) or A549 cells (C, D) were challenged for 2 hours with control medium or medium containing the indicated concentrations of pyolysin or streptolysin O. Cell viability was determined by MTT assay [open circles], and pore formation estimated by measuring the leakage of LDH [filled squares] into cell supernatants. The data are from four independent cell passages, and are presented as mean (SEM)

strongly with squalene synthase (Table 2), and 100 μM MPEX098 consistently protected HeLa cells against pyolysin as effectively as 10 μM Zaragozic acid, which is a reference squalene synthase inhibitor (Figure 4C). Treatment with 100 μM MPEX098 caused 8 ± 3% HeLa cell toxicity per se, and zaragozic acid caused 13 ± 3% cytotoxicity, as determined by MTT assay (Figure 4C, control challenge; n = 12). Cytoprotection against pyolysin was also evident within 6 hours of treating HeLa cells with 100 μM MPEX098 and plateaued at 16 to 24 hours (Figure 4D). We selected a 24 hour treatment with 100 μM MPEX098 as the candidate strategy to explore cytoprotection against cholesterol-dependent cytolysins.

3.5 | MPEX098 cytoprotection against cholesterol-dependent cytolysins

To examine the wider potential for MPEX098 to protect cells against cholesterol-dependent cytolysins, HeLa and A549 cells were treated for 24 hours with 100 μM MPEX098, and then challenged with a range of concentrations of pyolysin or streptolysin O. Treatment with MPEX098 protected HeLa cells against the detrimental effect of pyolysin on cell viability, and reduced the leakage of LDH (Figure 5A,C, $P < .001$). The >80% cytoprotection of HeLa cells against pyolysin or streptolysin O following treatment with 100 μM MPEX098 was similar to the > 90% cytoprotection of 10 μM zaragozic acid (Figure 5B,D: $P < .001$). This level of cytoprotection is also similar to the >70% cytoprotection against pyolysin or streptolysin O following treatment of HeLa cells with 10 μM atorvastatin, which is a statin that inhibits HMG-CoA reductase, or the >80% cytoprotection with 10 μM alendronate, which is a bisphosphonate that inhibits farnesyl diphosphate synthase (Supporting Information Figure S4). Both MPEX098 and zaragozic acid also protected A549 cells against a range of concentrations of streptolysin O (Figure 5E–H). Collectively, these results provide evidence that treating cells with 100 μM MPEX098 provides cytoprotection against cholesterol-dependent cytolysins.

3.6 | Validating MPEX098 cytoprotection against cholesterol-dependent cytolysins

We next sought additional evidence for the cytoprotective effects of MPEX098 against cholesterol-dependent cytolysins. Treatment with MPEX098 reduced the toxin-induced leakage of potassium from HeLa and A549 cells challenged with pyolysin and streptolysin O, respectively (Figure 6A-D).

Furthermore, when challenged with pyolysin, HeLa cells shrank, lost angularity, and lost definition of the cytoskeleton (Figure 7A,B). However, treatment with MPEX098 prevented these changes in the cells (Figure 7C,D), in a similar manner to the cholesterol-depleting agent methyl-β-cyclodextrin (Figure 7E,F), or zaragozic acid (Figure 7G,H).

Cells also mount stress responses when challenged with cholesterol-dependent cytolysins, typified by phosphorylation

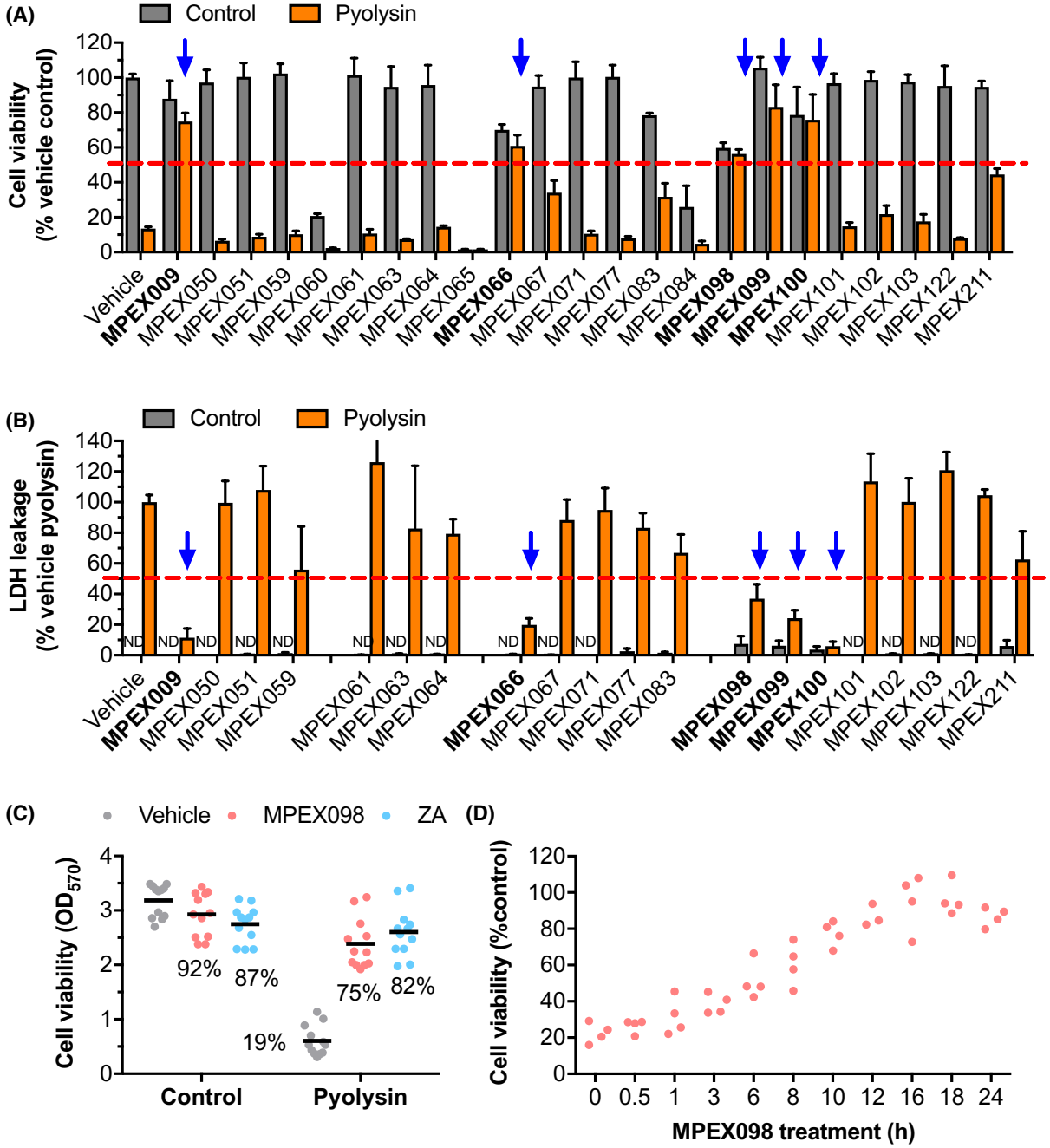

FIGURE 4 Screening nitrogen-containing bisphosphonates for cytoprotection against pyolysin. HeLa cells were treated for 24 hours with serum-free medium containing vehicle or 1 mM of the indicated bisphosphonic acid or ester, prior to 2 hours challenge with control medium or 2.5 μg/mL pyolysin. Cytoprotection against pyolysin was evaluated by MTT assay for cell viability and LDH assay for pore formation. The data are from three or four independent passages, and are presented as mean (SEM) percentage of vehicle challenged with control for cell viability (A), and vehicle challenged with pyolysin for LDH leakage (B; data not shown for cytotoxic bisphosphonates; ND, not detectable); the horizontal line marks the 50% level. Data were analyzed by ANOVA and compounds that show significant ($P < .05$) cytoprotection are in bold type and indicated by arrows. C, HeLa cells were treated for 24 hours with medium containing vehicle (●),100 μM MPEX098 (●) or 10 μM zaragozic acid (●), and then challenged for 2 hours with control medium or 2.5 μg/mL pyolysin. Cell viability was evaluated by MTT assay. The data are presented as dot plots, with each dot an independent cell passage (n = 12); the line represents the mean and the values are the percentage of control. D, HeLa cells were treated for the indicated times with medium containing vehicle (●) or 100 μM MPEX098 (●), or 10 μM zaragozic acid (●), and then challenged for 2 hours with control medium or 2.5 μg/mL pyolysin. Cell viability was evaluated by MTT assay. The data are from 4 independent experiments and presented as percentage of control, with each dot an independent measurement

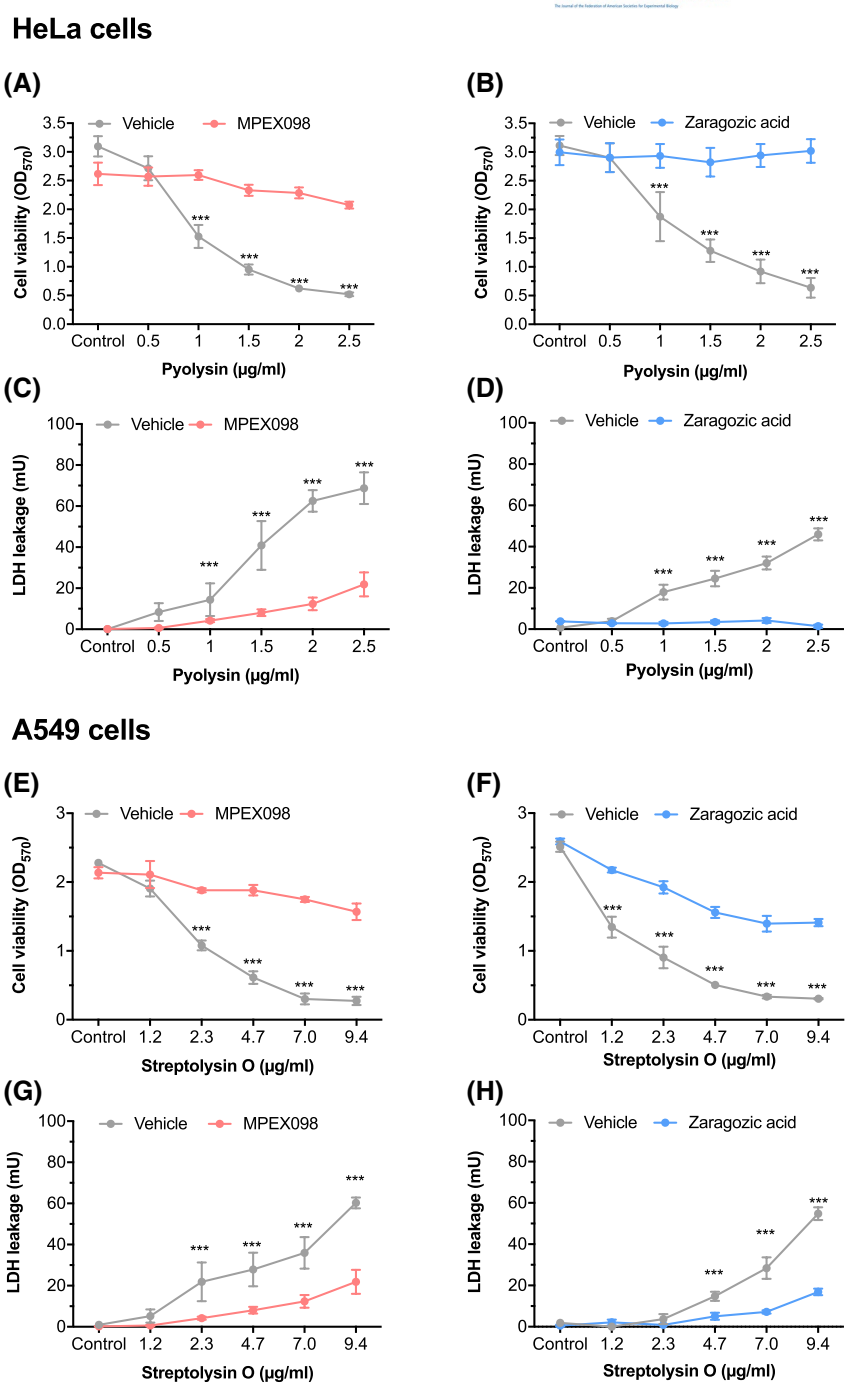

FIGURE 5 Squalene synthase inhibitors protect cells against cholesterol-dependent cytolysins. HeLa cells (A-D) or A549 cells (E-H) were treated for 24 hours with serum-free medium containing vehicle, 10 µM zaragozic acid (ZA), or 100 µM MPEX098. Cells were then challenged for 2 hours with control medium or the indicated concentrations of pyolysin or streptolysin O, and cell viability evaluated by MTT assay (A, B, E, F) and pore formation by measuring the leakage of LDH into cell supernatants (C, D, G, H). The data are from four independent passages, and are presented as mean (SEM). The data were analyzed by ANOVA with Dunnett post hoc test; within challenge values differ from vehicle, ***$P < .001$

of mitogen-activated protein kinases (MAPK).[10,52] However, treating HeLa cells with MPEX098 limited pyolysin-induced phosphorylation of MAPKs, ERK, JNK and p38, in a similar manner to zaragozic acid (Figure 8, Supporting Information Figures S5 and S6).

Whilst MPEX098 protected HeLa and A549 cells against cholesterol-dependent cytolysins, one concern was that these are immortal cell lines. Therefore, we examined if MPEX098 protected normal human dermal fibroblasts against pyolysin. Treatment with ≥250 µM MPEX098 protected the fibroblasts against cytolysis and reduced the leakage of LDH (Figure 9A,B). Treatment with MPEX098 also helped the fibroblasts maintain the shape of their actin cytoskeleton when challenged with pyolysin (Figure 9C).

3.7 | MPEX098 alters cholesterol biosynthesis

As inhibiting squalene synthase may limit cholesterol biosynthesis, cellular cholesterol was measured in HeLa and A549 cells incubated for 24 hours in serum-free media containing a range of concentrations of MPEX098. Cholesterol abundance was reduced by 100 µM MPEX098 in HeLa cells, and by

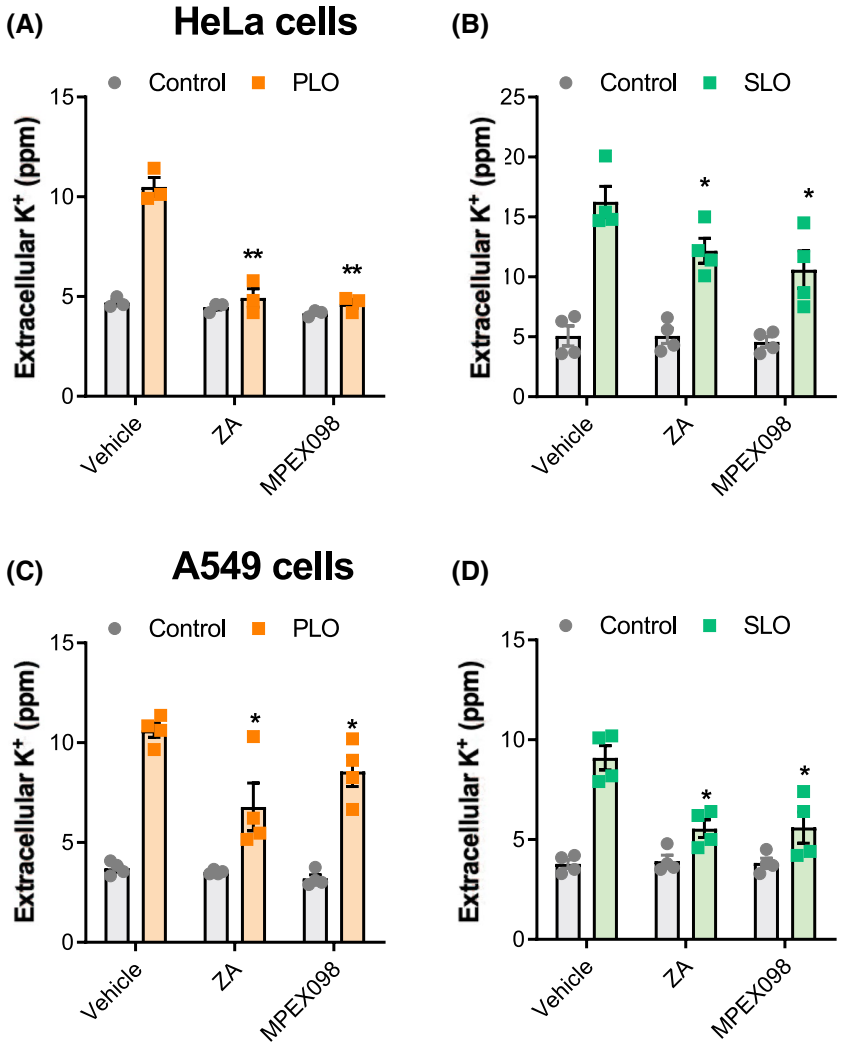

FIGURE 6 Treatment with squalene synthase inhibitors reduces potassium leakage. HeLa (A, B) or A549 (C, D) cells were treated for 24 hours in serum-free medium with vehicle, 10 μM zaragozic acid (ZA) or 100 μM MPEX098. Cells were then challenged with control choline buffer, or choline buffer containing 2.5 μg/mL pyolysin (A, C) or 9.4 μg/mL streptolysin O (B, D) for 10 minutes. Supernatants were collected and potassium concentrations measured using a flame photometer. The data are presented as mean (SEM) from 3 or 4 independent cell passages. The data were analyzed by ANOVA with Dunnett post hoc test; within SLO or PLO challenge values differ between treatments (ZA or MPEX098) and vehicle, * $P < .05$, ** $P < .01$

200 μM MPEX098 in A549 cells (Figure 10A,B). Using concentrations that protect cells against pyolysin, the reduction in HeLa cellular cholesterol was 36% for methyl-β-cyclodextrin, 25% for zaragozic acid and 15% for MPEX098 (Figure 10C). Further evidence for cholesterol depletion was provided by imaging cholesterol using filipin in HeLa cells (Figure 10D).

Reducing cholesterol biosynthesis by inhibiting squalene synthase also increases the accumulation of farnesyl diphosphate and geranylgeranyl diphosphate.[53] To test whether increased abundance of isoprenoids might also affect cytoprotection against cholesterol-dependent cytolysins, HeLa cells were treated with farnesyl diphosphate or geranylgeranyl diphosphate prior to challenge with pyolysin. Treatment with geranylgeranyl diphosphate but not farnesyl diphosphate ($P = .12$) increased cytoprotection against pyolysin (Figure 11).

4 | DISCUSSION

In the present study, we synthesized nitrogen-containing bisphosphonates that were designed to inhibit squalene synthase, and screened these compounds for cytoprotection against cholesterol-dependent cytolysins. Bisphosphonates contain a functional group with a similar structure to diphosphate and can inhibit farnesyl diphosphate synthase or squalene synthase.[28] Bisphosphonic inhibitors of farnesyl diphosphate synthase are widely used for the long-term treatment of osteoporosis, and have a high safety margin.[29] Although nitrogen-containing bisphosphonate inhibitors of squalene synthase are not effective against osteoporosis, we found that nitrogen-containing bisphosphonates protected cells against damage caused by cholesterol-dependent cytolysins, in a similar manner to the reference, zaragozic acid.[54,55]

We synthesized a library of 22 nitrogen-containing bisphosphonates using two approaches alongside the established bisphosphonate inhibitor of squalene synthase MPEX211 (PHPBP).[30,51] First, we used the method described by Goldeman et al,[32] whereby a series of isonitriles were treated with triethyl phosphite, undergoing an Arbuzov-like reaction to generate nitrogen-containing bisphosphonate esters that were subsequently hydrolyzed. As the synthesis of isonitriles is difficult on the milligram scale, and where isonitrile substrates were not commercially available, we used a second method, as described previously by Suzuki et al,[33] employing

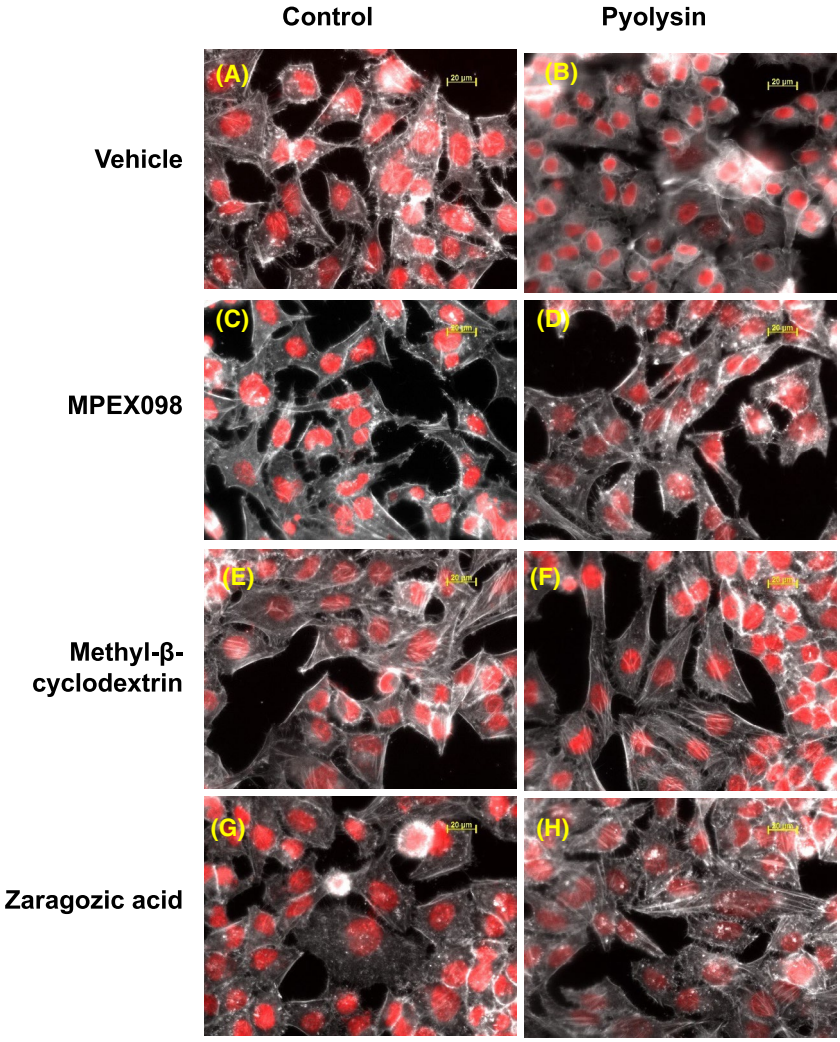

FIGURE 7 MPEX098 protects the actin cytoskeleton of HeLa cells challenged with pyolysin. HeLa cells were treated for 24 hours with serum-free medium containing vehicle (A, B), 100 µM MPEX098 (C, D), 1 mM methyl-β-cyclodextrin (E, F), or 10 µM zaragozic acid (G, H). The cells were then challenged for 2 hours with control medium (A, C, D, E) or 2.5 µg/mL pyolysin (B, D, F, H). Cells were fixed and stained using phalloidin-Alexa555 for actin (white) and DAPI for DNA (red). The images are representative of four independent experiments, and size markers are 20 µm

simple amines heated with triethylorthoformate and diethyl phosphite. We used both a cell-free squalene synthase assay and in silico docking to evaluate the ability of the synthesized bisphosphonates to inhibit squalene synthase. Three bisphosphonates had in silico affinity for the active site of squalene synthase that was similar to zaragozic acid. The cell-free assay was consistent with the DSX per contact score, which is a scoring function for ligand-protein interactions.[56]

Six nitrogen-containing bisphosphonates protected HeLa cells against pyolysin, and we selected MPEX098 as a lead compound because it inhibited squalene synthase in a cell-free assay, docked strongly with squalene synthase, and consistently protected HeLa cells against challenge with pyolysin at a concentration of 100 µM. Several lines of evidence supported the cytoprotective effect of MPEX098 against pyolysin. First, treating cells with MPEX098 reduced the formation of pores when cells were challenged with pyolysin, as determined by reduced leakage of potassium ions and lactate dehydrogenase. Second, treating cells with MPEX098 reduced the expected MAPK stress response to pores formed by cholesterol-dependent cytolysins.[8,10,52,57] Third, MPEX098 treatment prevented the expected pyolysin-induced changes in cell viability and the actin cytoskeleton, which are likely caused by the pores in plasma membranes leading to alterations in osmotic tension.[58] Finally, MPEX098 also protected A549 human lung epithelial cells and primary human dermal fibroblasts against pyolysin, and protected HeLa cells against Streptolysin O. Although the concentration of MPEX098 needed for cytoprotection was ten-fold higher than zaragozic acid, the IC_{50} of MPEX098 was 0.41 µM in a squalene synthase cell free assay, whereas the IC_{50} of zaragozic acid was 0.012 µM.[59] The IC_{50} of MPEX098 is similar to other bisphosphonic inhibitors of squalene synthase.[28,60] The higher concentrations of MPEX098 and zaragozic acid needed to protect cells than implied by the IC_{50} values may reflect lower bioavailability or reduced lipophilicity, which prevents transcellular transport across the epithelial barriers.[61] Zaragozic acid also caused cytotoxicity *per se* at 10 µM, compared with the 100 µM to 1 mM cytotoxic concentration for the bisphosphonates.

Most cholesterol is located in the plasma membrane, where there are three functional pools of cholesterol: an essential pool, a sphingomyelin-bound pool, and a pool of

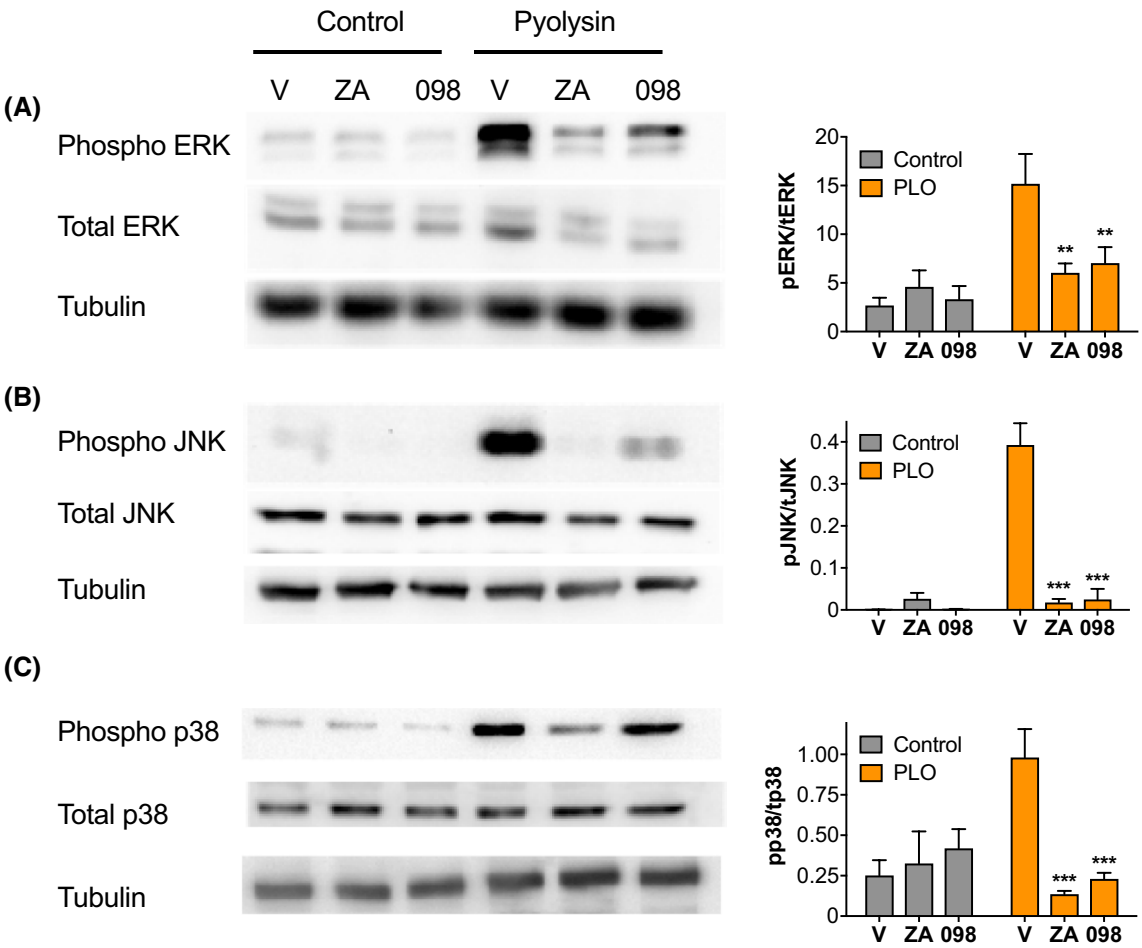

FIGURE 8 Squalene synthase inhibitors alter MAPK phosphorylation. HeLa cells were treated for 24 hours with serum-free medium containing vehicle (V), 10 μM zaragozic acid (ZA) or 100 μM MPEX098 (098), prior to a 10 minutes challenge with control medium or medium containing 2.5 μg/well pyolysin (PLO). Cells were then collected for Western blotting for phosphorylated and total ERK and tubulin (A), phosphorylated and total JNK and tubulin (B), or phosphorylated and total p38 and tubulin (C). Representative images of four independent experiments are presented (left panel), and densitometry was performed on the blots [right panel] with data presented as mean (SEM) of the ratio of phosphorylated to total protein, normalized to tubulin, Within PLO challenge values differ between treatments (ZA or MPEX098) and vehicle
** $P < .01$, *** $P < .001$

"labile" accessible cholesterol.[62] Accessible cholesterol is bound by cholesterol-dependent cytolysins, usually when there is >35 mol% cholesterol in membranes.[62,63] Thus, an obvious mechanism for protecting cells against cholesterol-dependent cytolysins is reducing the abundance of accessible cholesterol, using compounds such as cyclodextrins or zaragozic acid.[2,53,64–66] For example, treatment with cyclodextrins or zaragozic acid protects fibroblasts against pyolysin.[54] Compared with cyclodextrins or zaragozic acid, MPEX098 only reduced cholesterol in HeLa and A549 cells by 15% at most. This modest reduction may be sufficient to alter the accessible pool of cholesterol in the plasma membrane.[62,67] A potential alternative mechanism is via changes in isoprenoids because inhibiting squalene synthase increases the concentration of cellular farnesyl diphosphate and geranylgeranyl diphosphate.[53,68,69] Unfortunately, it is technically challenging to robustly measure cellular isoprenoids.[70] Therefore, in the present study, we examined the effect of treatment with isoprenoids, and we found that geranylgeranyl diphosphate protected cells against pyolysin. One possibility is that geranylgeranyl diphosphate may help sustain the actin cytoskeleton as alcohol derivatives of geranylgeranyl diphosphate affect the actin cytoskeleton via prenylation of Rho.[68] Another possibility is changes in cellular cholesterol because geranylgeranyl diphosphate is a reverse agonist for Liver X receptors, which regulate the expression of squalene synthase and cholesterol efflux.[71–73] However, there are other potential mechanisms, including changes in oxysterols as increasing 25-hydroxycholesterol protects cells against cholesterol-dependent cytolysins, without altering cholesterol abundance.[74]

Cytoprotection using MPEX098 may be able to protect tissues against pathogenic bacteria that secrete cholesterol-dependent cytolysins. Defense against pathogenic bacteria

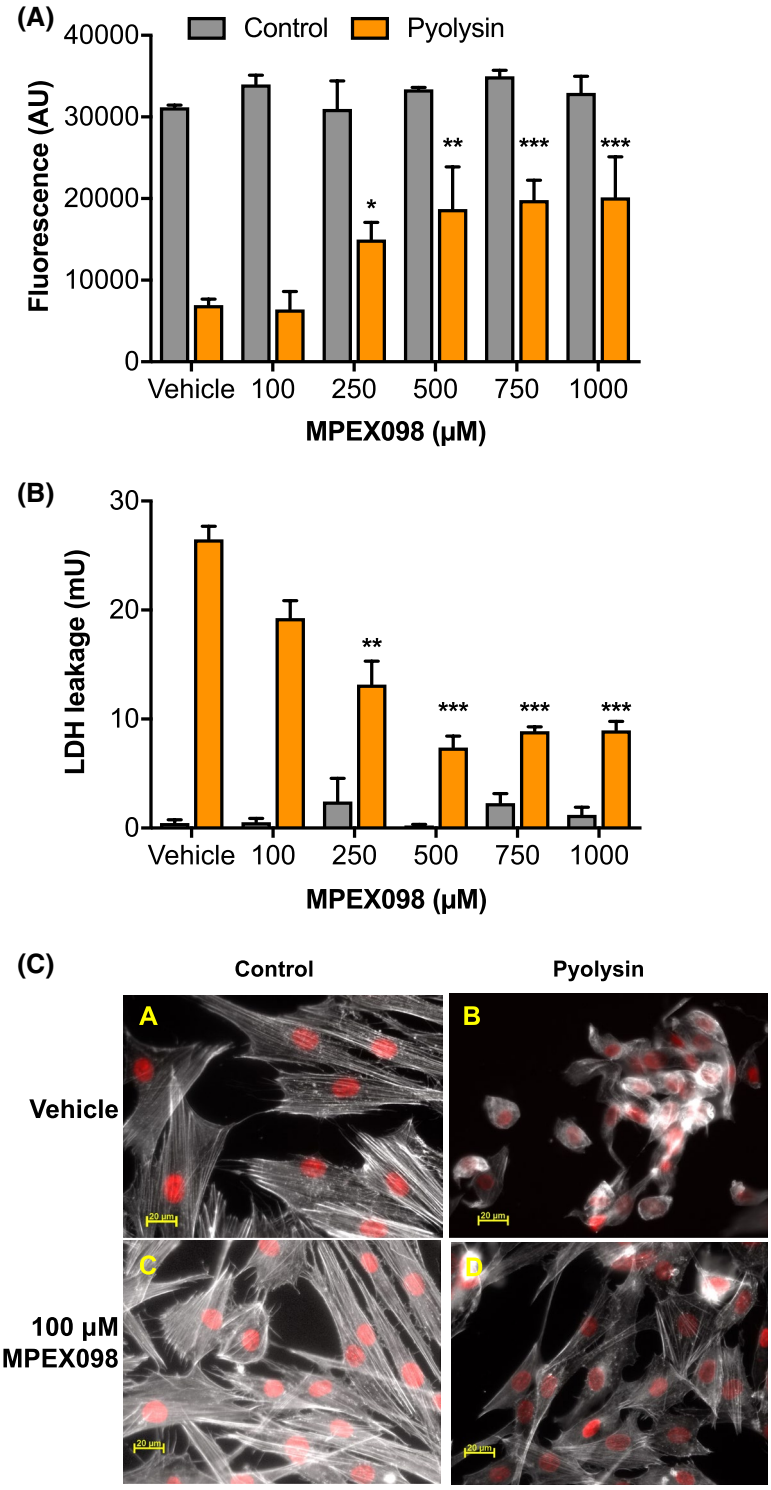

FIGURE 9 MPEX098 protects primary cells against pyolysin. Dermal fibroblasts were treated for 48 hours with serum-free medium containing vehicle or the indicated concentrations of MPEX098. Cells were then challenged for 2 hours with control medium or medium containing 1 μg/mL pyolysin. Cell viability was measured using Alamar Blue (A), and pore formation estimated by LDH leakage into cell supernatants (B). The data are from four independent cell passages, and presented as mean (SEM). The data were analyzed by ANOVA with Dunnett's multiple comparison post hoc test; within challenge, values differ from vehicle, $*P < .05$, $**P < .01$, $***P < .001$. C, Cells were fixed and stained for actin using phalloidin-Alexa555 (White) and DNA (Red). Images are representative of four independent passages

depends on resisting and tolerating infections.[75,76] Resistance is the function of immunity or antimicrobials, which aim to kill bacteria to limit the pathogen burden.[63,75] Tolerance is the ability to limit the tissue damage caused by the pathogens.[77] Tolerance mechanisms include neutralizing bacterial toxins and protecting cells against damage. Increasing tolerance to pathogenic bacteria is an attractive strategy because this reduces the risk of antimicrobial resistance. In particular, it may be possible to apply treatments parenterally, or directly to mucosae or skin, to prevent tissue damage caused by pathogenic bacteria that secrete cholesterol-dependent cytolysins. For example, an intra-uterine infusion of a drug to reduce endometrial cellular cholesterol might protect against pyolysin-induced damage and help prevent postpartum uterine disease in cattle caused by *T. pyogenes*, instead of using antibiotic treatments.[2,13] Similarly, applying treatments via a spray or lozenge to the oropharynx that reduced pharyngeal epithelial cell cholesterol might protect against the 37% of

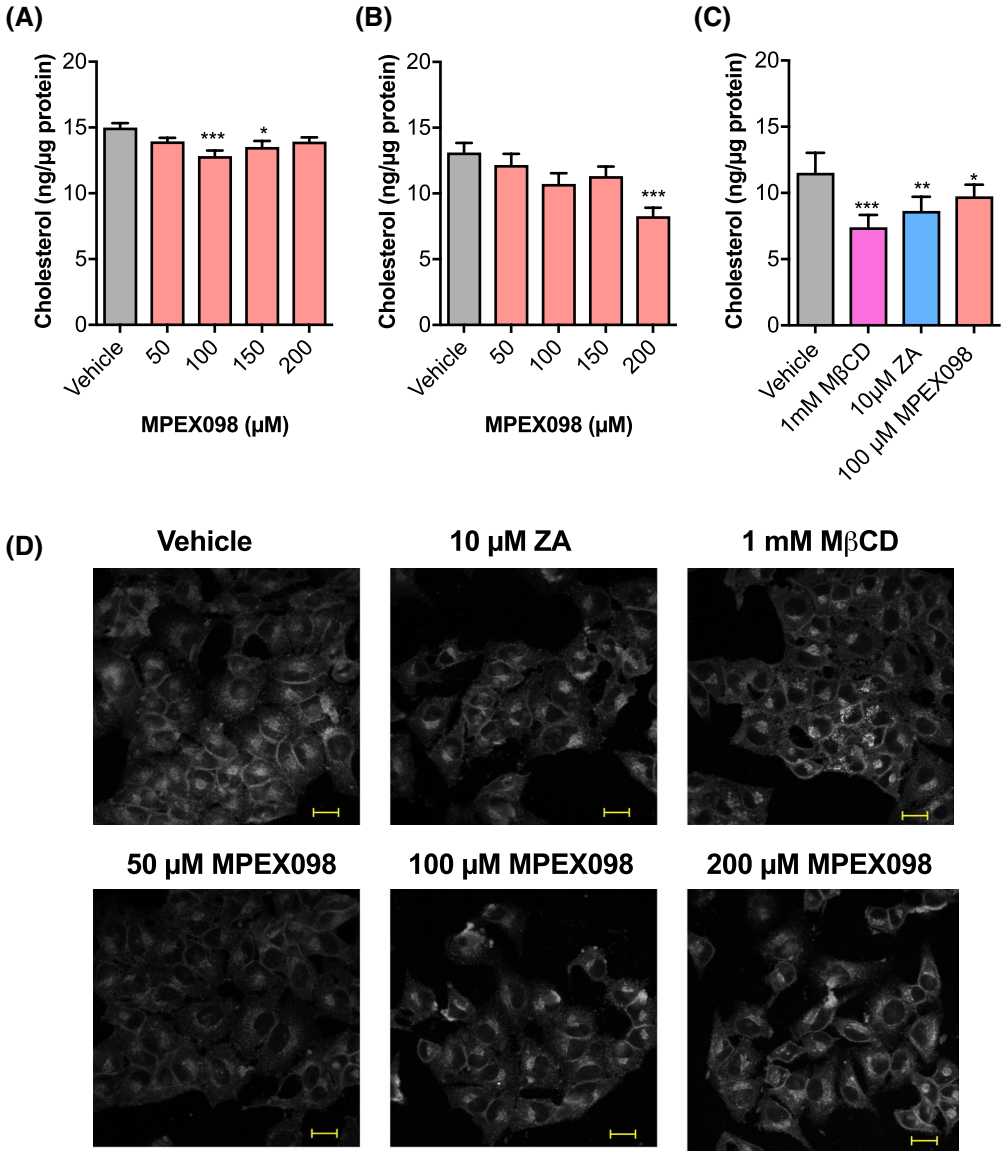

FIGURE 10 MPEX098 reduces cellular cholesterol. HeLa (A, C) or A549 (B) cells were treated for 24 hours with vehicle or the indicated concentrations of MPEX098, 1 mM methyl-β-cyclodextrin (MβCD), or 10 µM zaragozic acid (ZA) in serum-free medium, and cholesterol and protein quantified. The data are presented as mean (SEM) from ≥ 4 independent cell passages, and were analyzed by ANOVA with Dunnett's post hoc test; values differ from vehicle, *$P < .05$, ** $P < .01$, *** $P < .001$. D, HeLa cells were stained with filipin for cholesterol and images acquired using 40× objective and 340 nm excitation and 480 nm emission filters. Representative images of four independent experiments are shown. Scale bars are 20 µm

cases of pharyngitis associated with group A *Streptococci* in children.[14]

The present work extends previous findings that statins protect cells against vaginolysin and pneumolysin.[3,23,78,79] While both reduce cholesterol synthesis, statins and nitrogen-containing bisphosphonates differ in their action, depleting or increasing isoprenoids, respectively. Furthermore inhibiting squalene synthase may prevent squalene being a feedforward stimulus for cholesterol biosynthesis.[80] The action of statins is also complicated by their lipophilic properties, whereby lipophilic simvastatin is more cytoprotective than hydrophilic pravastatin, independent of changes in cellular cholesterol, and may instead be associated with altering lipid raft composition and organization.[79] In future work, it would be interesting to explore whether nitrogen-containing bisphosphonates targeting squalene synthase also affect membrane lipid rafts.

In conclusion, the present study explored the cytoprotective effect of nitrogen-containing bisphosphonates, which were designed to inhibit squalene synthase to protect cells against cholesterol-dependent cytolysins. Although the mechanism of action remains elusive, we provide several lines of evidence that our lead bisphosphonate, MPEX098, provided cytoprotection against cholesterol-dependent cytolysins. These findings imply that nitrogen-containing

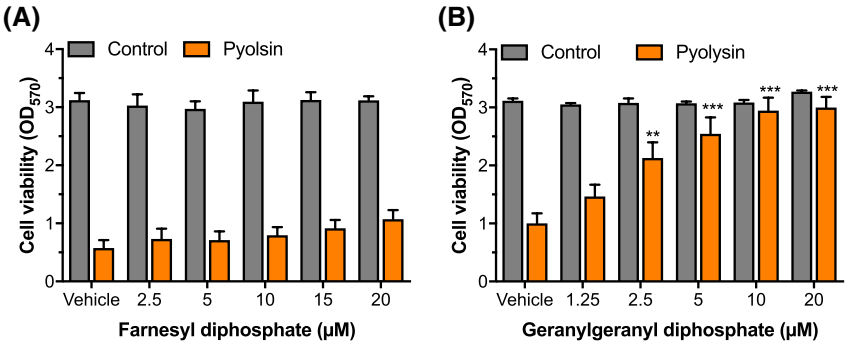

FIGURE 11 Isoprenoids and cytoprotection against pyolysin. HeLa cells were treated for 24 hours with serum-free medium containing vehicle or the indicated concentrations of the isoprenoids farnesyl diphosphate (A) or geranylgeranyl diphosphate (B). Cells were then challenged for 2 hours with control medium or 2.5 μg/mL pyolysin (PLO), and cell viability measured by MTT assay. The data are from four independent passages, and are presented as mean (SEM). The data were analyzed by ANOVA with Dunnett's multiple comparison post hoc test; within challenge, values differ from vehicle, $^{**}P < .01$, $^{***}P < .001$

bisphosphonates might help protect tissues against pathogenic bacteria that secrete cholesterol-dependent cytolysins.

ACKNOWLEDGMENTS

This work was funded by the Sêr Cymru National Research Network of the Welsh Government.

CONFLICT OF INTEREST

No conflicts of interest are present in connection with this article.

AUTHOR CONTRIBUTIONS

I. M. Sheldon, R. K. Allemann, and M. Pospiech designed the research; M. Pospiech performed most of the research and analyzed data; J. G. Cronin, S. E. Owens, and D. Miller contributed to the methodology; K. Austin-Muttitt and J. G. L. Mullins performed docking studies; M. Pospiech and I. M. Sheldon wrote the paper.

ORCID

Mateusz Pospiech https://orcid.org/0000-0002-7425-8800
I. Martin Sheldon https://orcid.org/0000-0001-7902-5558

REFERENCES

1. Peraro MD, van der Goot FG. Pore-forming toxins: ancient, but never really out of fashion. *Nat Rev Microbiol*. 2016;14(2):77-92.
2. Amos MR, Healey GD, Goldstone RJ, et al. Differential endometrial cell sensitivity to a cholesterol-dependent cytolysin links *Trueperella pyogenes* to uterine disease in cattle. *Biol Reprod*. 2014;90(3):1-13.
3. Statt S, Ruan J-W, Hung L-Y, et al. Statin-conferred enhanced cellular resistance against bacterial pore-forming toxins in airway epithelial cells. *Am J Respir Cell Mol Biol*. 2015;53(5):689-702.
4. Tan JMJ, Mellouk N, Osborne SE, et al. An ATG16L1-dependent pathway promotes plasma membrane repair and limits *Listeria monocytogenes* cell-to-cell spread. *Nat Microbiol*. 2018;3(12):1472-1485.
5. Tweten RK. Cholesterol-dependent cytolysins, a family of versatile pore-forming toxins. *Infect Immun*. 2005;73(10):6199-6209.
6. Waheed AA, Shimada Y, Heijnen HFG, et al. Selective binding of perfringolysin O derivative to cholesterol-rich membrane microdomains (rafts). *PNAS*. 2001;98(9):4926-4931.
7. Gonzalez MR, Bischofberger M, Frêche B, Ho S, Parton RG, van der Goot FG. Pore-forming toxins induce multiple cellular responses promoting survival. *Cell Microbiol*. 2011;13(7):1026-1043.
8. Gurcel L, Abrami L, Girardin S, Tschopp J, van der Goot FG. Caspase-1 activation of lipid metabolic pathways in response to bacterial pore-forming toxins promotes cell survival. *Cell*. 2006;126(6):1135-1145.
9. Keyel PA, Loultcheva L, Roth R, et al. Streptolysin O clearance through sequestration into blebs that bud passively from the plasma membrane. *J Cell Sci*. 2011;124(14):2414-2423.
10. Preta G, Lotti V, Cronin JG, Sheldon IM. Protective role of the dynamin inhibitor Dynasore against the cholesterol-dependent cytolysin of *Trueperella pyogenes*. *FASEB J*. 2015;29(4):1516-1528.
11. Bhakdi S, Tranum-Jensen J, Sziegoleit A. Mechanism of membrane damage by streptolysin-O. *Infect Immun*. 1985;47(1):52-60.
12. Jost BH, Billington SJ. *Arcanobacterium pyogenes*: molecular pathogenesis of an animal opportunist. *Antonie Van Leeuwenhoek*. 2005;88(2):87-102.
13. Sheldon IM, Cronin JG, Bromfield JJ. Tolerance and innate immunity shape the development of postpartum uterine disease and the impact of endometritis in dairy cattle. *Annu Rev Anim Biosci*. 2019;7:361-384.
14. Shaikh N, Leonard E, Martin JM. Prevalence of streptococcal pharyngitis and streptococcal carriage in children: a meta-analysis. *Pediatrics*. 2010;126(3):e557-e564.
15. Pleckaityte M. Cholesterol-dependent cytolysins produced by vaginal bacteria: certainties and controversies. *Front Cell Infect Microbiol*. 2020;9:1-14.
16. Sierig G, Cywes C, Wessels MR, Ashbaugh CD. Cytotoxic effects of streptolysin O and streptolysin S enhance the virulence of poorly encapsulated group a streptococci. *Infect Immun*. 2003;71(1):446-455.
17. Hirst RA, Kadioglu A, O'callaghan C, Andrew PW. The role of pneumolysin in pneumococcal pneumonia and meningitis. *Clin Exp Immunol*. 2004;138(2):195-201.

18. Billington SJ, Jost BH, Songer JG. Thiol-activated cytolysins: structure, function and role in pathogenesis. *FEMS Microbiol Lett*. 2000;182(2):197-205.
19. Alouf JE. Streptococcal toxins (streptolysin O, streptolysin S, erythrogenic toxin). *Pharmacol Ther*. 1980;11(3):661-717.
20. McCarville J, Ayres J. Disease tolerance: concept and mechanisms. *Curr Opin Immunol*. 2018;50:88-93.
21. Read AF, Graham AL, Råberg L. Animal defenses against infectious agents: is damage control more important than pathogen control. *PLoS Biol*. 2008;6(12):e1000004.
22. Goldstein JL, Brown MS. Regulation of the mevalonate pathway. *Nature*. 1990;343:425-430.
23. Abdelmaksoud AA, Girerd PH, Garcia EM, et al. Association between statin use, the vaginal microbiome, and *Gardnerella vaginalis* vaginolysin-mediated cytotoxicity. *PLoS One*. 2017;12(8):e0183765.
24. Tansey TR, Shechter I. Structure and regulation of mammalian squalene synthase. *Biochim Biophys Acta Mol Cell Biol Lipids*. 2000;1529(1):49-62.
25. Amin D, Rutledge RZ, Needle SN, et al. RPR 107393, a potent squalene synthase inhibitor and orally effective cholesterol-lowering agent: comparison with inhibitors of HMG-CoA reductase. *J Pharmacol Exp Ther*. 1997;281(2):746-752.
26. Bergstrom JD, Kurtz MM, Rew DJ, et al. Zaragozic acids: a family of fungal metabolites that are picomolar competitive inhibitors of squalene synthase. *PNAS*. 1993;90(1):80-84.
27. Ichikawa M, Yokomizo A, Itoh M, et al. Discovery of atrop fixed alkoxy-aminobenzhydrol derivatives: novel, highly potent and orally efficacious squalene synthase inhibitors. *Bioorg Med Chem*. 2011;19(17):5207-5224.
28. Ciosek CP, Magnin DR, Harrity TW, et al. Lipophilic 1,1-bisphosphonates are potent squalene synthase inhibitors and orally active cholesterol lowering agents in vivo. *J Biol Chem*. 1993;268(33):24832-24837.
29. Rogers MJ. From molds and macrophages to mevalonate: a decade of progress in understanding the molecular mode of action of bisphosphonates. *Calcif Tissue Int*. 2004;75(6):451-461.
30. Amin D, Cornell SA, Gustafson SK, et al. Bisphosphonates used for the treatment of bone disorders inhibit squalene synthase and cholesterol biosynthesis. *J Lipid Res*. 1992;33(11):1657-1663.
31. Wasko BM, Smits JP, Shull LW, Wiemer DF, Hohl RJ. A novel bisphosphonate inhibitor of squalene synthase combined with a statin or a nitrogenous bisphosphonate in vitro. *J Lipid Res*. 2011;52(11):1957-1964.
32. Goldeman W, Kluczyński A, Soroka M. The preparation of N-substituted aminomethylidenebisphosphonates and their tetraalkyl esters via reaction of isonitriles with trialkyl phosphites and hydrogen chloride. Part 1. *Tetrahedron Lett*. 2012;53(39):5290-5292.
33. Suzuki F, Fujikawa Y, Yamamoto S, et al. *N-pyridylaminomethy lendiphosphonsaeureverbindungen*. Published online February 1, 1979. Accessed August 3, 2020. https://patents.google.com/patent/DE2831578A1/de
34. McKenna CE, Schmidhuser J. Functional selectivity in phosphonate ester dealkylation with bromotrimethylsilane. *J Chem Soc, Chem Commun*. 1979;17:739.
35. Agnew WS, Popják G. Squalene synthetase. Solubilization from yeast microsomes of a phospholipid-requiring enzyme. *J Biol Chem*. 1978;253(13):4574-4583.
36. Tait RM. Development of a radiometric spot-wash assay for squalene synthase. *Anal Biochem*. 1992;203(2):310-316.
37. Thompson JF, Danley DE, Mazzalupo S, Milos PM, Lira ME, Harwood HJ. Truncation of human squalene synthase yields active, crystallizable protein. *Arch Biochem Biophys*. 1998;350(2):283-290.
38. Pettersen EF, Goddard TD, Huang CC, et al. UCSF Chimera—a visualization system for exploratory research and analysis. *J Comput Chem*. 2004;25(13):1605-1612.
39. Wang J, Wang W, Kollman PA, Case DA. Automatic atom type and bond type perception in molecular mechanical calculations. *J Mol Graph Model*. 2006;25(2):247-260.
40. Kuntz ID, Blaney JM, Oatley SJ, Langridge R, Ferrin TE. A geometric approach to macromolecule-ligand interactions. *J Mol Biol*. 1982;161(2):269-288.
41. Meng EC, Shoichet BK, Kuntz ID. Automated docking with grid-based energy evaluation. *J Comput Chem*. 1992;13(4):505-524.
42. Volkamer A, Kuhn D, Grombacher T, Rippmann F, Rarey M. Combining global and local measures for structure-based druggability predictions. *J Chem Inf Model*. 2012;52(2):360-372.
43. O'Boyle NM, Banck M, James CA, Morley C, Vandermeersch T, Hutchison GR. Open Babel: an open chemical toolbox. *J Cheminform*. 2011;3(1):1-14.
44. Vainio MJ, Johnson MS. Generating conformer ensembles using a multiobjective genetic algorithm. *J Chem Inf Model*. 2007;47(6):2462-2474.
45. Geidl S, Bouchal T, Raček T, et al. High-quality and universal empirical atomic charges for chemoinformatics applications. *J Cheminformatics*. 2015;7(1):1-10.
46. Allen WJ, Balius TE, Mukherjee S, et al. DOCK 6: impact of new features and current docking performance. *J Comput Chem*. 2015;36(15):1132-1156.
47. Trott O, Olson AJ. AutoDock Vina: improving the speed and accuracy of docking with a new scoring function, efficient optimization, and multithreading. *J Comput Chem*. 2010;31(2):455-461.
48. Page B, Page M, Noel C. A new fluorometric assay for cytotoxicity measurements in-vitro. *Int J Oncol*. 1993;3(3):473-476.
49. Maxfield FR, Wüstner D. Analysis of cholesterol trafficking with fluorescent probes. *Methods Cell Biol*. 2012;108:367-393.
50. Kurzak B, Goldeman W, Szpak M, Matczak-Jon E, Kamecka A. Synthesis of N-methyl alkylaminomethane-1,1-diphosphonic acids and evaluation of their complex-formation abilities towards copper(II). *Polyhedron*. 2015;85:675-684.
51. Widler L, Jaeggi KA, Glatt M, et al. Highly potent geminal bisphosphonates. From pamidronate disodium (Aredia) to zoledronic acid (Zometa). *J Med Chem*. 2002;45(17):3721-3738.
52. Huffman DL, Abrami L, Sasik R, Corbeil J, van der Goot FG, Aroian RV. Mitogen-activated protein kinase pathways defend against bacterial pore-forming toxins. *PNAS*. 2004;101(30):10995-11000.
53. Keller RK. Squalene synthase inhibition alters metabolism of nonsterols in rat liver. *Biochim Biophys Acta Mol Cell Biol Lipid*. 1996;1303(3):169-179.
54. Griffin S, Preta G, Sheldon IM. Inhibiting mevalonate pathway enzymes increases stromal cell resilience to a cholesterol-dependent cytolysin. *Sci Rep*. 2017;7(1):17050.
55. Griffin S, Healey GD, Sheldon IM. Isoprenoids increase bovine endometrial stromal cell tolerance to the cholesterol-dependent cytolysin from *Trueperella pyogenes*. *Biol Reprod*. 2018;99(4):749-760.
56. Neudert G, Klebe G. DSX: A knowledge-based scoring function for the assessment of protein–ligand complexes. *J Chem Inf Model*. 2011;51(10):2731-2745.

57. Magnin DR, Dickson JK, Logan JV, et al. 1,1-Bisphosphonate squalene synthase inhibitors: interplay between the isoprenoid subunit and the diphosphate surrogate. *J Med Chem*. 1995;38(14):2596-2605.
58. Lin JH. Bisphosphonates: a review of their pharmacokinetic properties. *Bone*. 1996;18(2):75-85.
59. Kao C-Y, Los FCO, Huffman DL, et al. Global functional analyses of cellular responses to pore-forming toxins. *PLoS Pathog*. 2011;7(3):e1001314.
60. Boucher E, Mandato CA. Plasma membrane and cytoskeleton dynamics during single-cell wound healing. *Biochim Biophys Acta Mol Cell Res*. 2015;1853(10, Part A):2649-2661.
61. Baxter A, Fitzgerald BJ, Hutson JL, et al. Squalestatin 1, a potent inhibitor of squalene synthase, which lowers serum cholesterol in vivo. *J Biol Chem*. 1992;267(17):11705-11708.
62. Das A, Brown MS, Anderson DD, Goldstein JL, Radhakrishnan A. Three pools of plasma membrane cholesterol and their relation to cholesterol homeostasis. Young SG ed. *eLife*. 2014;3:e02882.
63. Das A, Goldstein JL, Anderson DD, Brown MS, Radhakrishnan A. Use of mutant 125I-Perfringolysin O to probe transport and organization of cholesterol in membranes of animal cells. *PNAS*. 2013;110(26):10580-10585.
64. Bergstrom JD, Dufresne C, Bills GF, Nallin-Omstead M, Byrne K. Discovery, biosynthesis, and mechanism of action of the zaragozic acids: potent inhibitors of squalene synthase. *Annu Rev Microbiol*. 1995;49:607-639.
65. Giddings KS, Johnson AE, Tweten RK. Redefining cholesterol's role in the mechanism of the cholesterol-dependent cytolysins. *PNAS*. 2003;100(20):11315-11320.
66. Iliev AI, Djannatian JR, Nau R, Mitchell TJ, Wouters FS. Cholesterol-dependent actin remodeling via RhoA and Rac1 activation by the *Streptococcus pneumoniae* toxin pneumolysin. *PNAS*. 2007;104(8):2897-2902.
67. Keller RK, Mitchell DA, Goulah CC, Fliesler SJ. Hepatic isoprenoid metabolism in a rat model of Smith-Lemli-Opitz syndrome. *Lipids*. 2013;48(3):219-229.
68. Miquel K, Pradines A, Favre G. Farnesol and geranylgeraniol induce actin cytoskeleton disorganization and apoptosis in A549 lung adenocarcinoma cells. *Biochem Biophys Res Commu*. 1996;225(3):869-876.
69. Wang Y, Muneton S, Sjövall J, Jovanovic JN, Griffiths WJ. The effect of 24S-hydroxycholesterol on cholesterol homeostasis in neurons: quantitative changes to the cortical neuron proteome. *J Proteome Res*. 2008;7(4):1606-1614.
70. Fukuchi J, Song C, Ko AL, Liao S. Transcriptional regulation of farnesyl pyrophosphate synthase by liver X receptors. *Steroids*. 2003;68(7):685-691.
71. Kandutsch AA, Chen HW. Inhibition of sterol synthesis in cultured mouse cells by cholesterol derivatives oxygenated in the side chain. *J Biol Chem*. 1974;249(19):6057-6061.
72. Repa JJ, Turley SD, Lobaccaro J-MA, et al. Regulation of absorption and ABC1-mediated efflux of cholesterol by RXR heterodimers. *Science*. 2000;289(5484):1524-1529.
73. Zhou QD, Chi X, Lee MS, et al. Interferon-mediated reprogramming of membrane cholesterol to evade bacterial toxins. *Nat Immunol*. 2020;21(7):746-755.
74. Abrams ME, Johnson KA, Perelman SS, et al. Oxysterols provide innate immunity to bacterial infection by mobilizing cell surface accessible cholesterol. *Nat Microbiol*. 2020;5(7):929-942.
75. Ayres JS, Schneider DS. Tolerance of infections. *Annu Rev Immunol*. 2012;30(1):271-294.
76. Soares MP, Teixeira L, Moita LF. Disease tolerance and immunity in host protection against infection. *Nat Rev Immunol*. 2017;17(2):83-96.
77. Råberg L, Sim D, Read AF. Disentangling genetic variation for resistance and tolerance to infectious diseases in animals. *Science*. 2007;318(5851):812-814.
78. Yoshioka H, Coates HW, Chua NK, Hashimoto Y, Brown AJ, Ohgane K. A key mammalian cholesterol synthesis enzyme, squalene monooxygenase, is allosterically stabilized by its substrate. *PNAS*. 2020;117(13):7150-7158.
79. Zhang DL, Jennings SM, Robinson GW, Poulter CD. Yeast squalene synthase: expression, purification, and characterization of soluble recombinant enzyme. *Arch Biochem Biophys*. 1993;304(1):133-143.
80. Radisky ES, Poulter CD. Squalene synthase: steady-state, pre-steady-state, and isotope-trapping studies. *Biochemistry*. 2000;39(7):1748-1760.

SUPPORTING INFORMATION

Additional Supporting Information may be found online in the Supporting Information section.

How to cite this article: Pospiech M, Owens SE, Miller DJ, et al. Bisphosphonate inhibitors of squalene synthase protect cells against cholesterol-dependent cytolysins. *The FASEB Journal*. 2021;35:e21640. https://doi.org/10.1096/fj.202100164R